



저작자표시-비영리-변경금지 2.0 대한민국

이용자는 아래의 조건을 따르는 경우에 한하여 자유롭게

- 이 저작물을 복제, 배포, 전송, 전시, 공연 및 방송할 수 있습니다.

다음과 같은 조건을 따라야 합니다:



저작자표시. 귀하는 원저작자를 표시하여야 합니다.



비영리. 귀하는 이 저작물을 영리 목적으로 이용할 수 없습니다.



변경금지. 귀하는 이 저작물을 개작, 변형 또는 가공할 수 없습니다.

- 귀하는, 이 저작물의 재이용이나 배포의 경우, 이 저작물에 적용된 이용허락조건을 명확하게 나타내어야 합니다.
- 저작권자로부터 별도의 허가를 받으면 이러한 조건들은 적용되지 않습니다.

저작권법에 따른 이용자의 권리는 위의 내용에 의하여 영향을 받지 않습니다.

이것은 [이용허락규약\(Legal Code\)](#)을 이해하기 쉽게 요약한 것입니다.

[Disclaimer](#)

약학석사학위논문

**Target deconvolution of active  
molecules to regulate adipogenesis in  
human mesenchymal stem cells**

사람의 중간엽줄기세포에서 지방분화 조절 물질의  
타겟 규명

2017 년 2 월

서울대학교 약학대학원  
약학과 천연물과학전공

안 세 연

## ABSTRACT

# Target deconvolution of active molecules to regulate adipogenesis in human mesenchymal stem cells

Seyeon Ahn

Department of Pharmacy

The Graduate School of Pharmacy

Seoul National University

IB-MECA and its structural analogs, A<sub>3</sub> adenosine receptor (AR) agonists have been clinically developed to treat human diseases such as hepatocellular carcinoma, psoriasis and rheumatoid arthritis. Recently, the effects of ARs on metabolic disease such as type II diabetes and obesity have been also studied.

One of phenotype-based assays, the induction of adipogenesis in human bone marrow mesenchymal stem cells (hBM-MSCs) is utilized to drug screening for metabolic diseases. IB-MECA promoted the production of adiponectin during adipogenesis in hBM-MSCs, associated with the improvement of insulin sensitivity. Its structural analogs, both A<sub>3</sub> AR agonists and A<sub>3</sub> AR antagonists showed similar activities in hBM-MSCs indicating adipogenesis is mediated by off-target. In a target deconvolution study, IB-MECA and its structural analogs have binding

activities to both peroxisome proliferator activated receptor (PPAR) $\gamma$  and PPAR $\delta$ . The important thing is that the adiponectin-promoting activity of IB-MECA and its structural analogs significantly correlated with PPAR $\gamma$  and PPAR $\delta$  binding affinity. Conclusively, we elucidated that IB-MECA and its structural analogs play roles as both PPAR $\gamma$  partial agonists and PPAR $\delta$  antagonists. In the streptozotocin (STZ)-induced diabetic C57BL/6J mice model, the most potent IB-MECA structural analog significantly improved serum glucose and triglyceride indicating anti-diabetic potential. Together, our finding reveals that the polypharmacological feature of IB-MECA and its structural analogs suggests a therapeutic insight against human metabolic diseases.

**keywords :** Polypharmacology, IB-MECA, Human bone marrow mesenchymal stem cells, Phenotype screening, Target deconvolution, Adipogenesis

***Student number :*** 2015-21884

# CONTENTS

<b>ABSTRACT</b> .....	<b>1</b>
<b>TABLE OF CONTENTS</b> .....	<b>3</b>
<b>LIST OF FIGURES</b> .....	<b>5</b>
<b>LIST OF TABLES</b> .....	<b>7</b>
<b>I . Introduction</b> .....	<b>8</b>
<b>II . Materials and Methods</b> .....	<b>11</b>
1. Cell culture and differentiation.....	11
2. Enzyme-linked immunosorbent assay (ELISA) .....	11
3. Nuclear receptor (NR) assays .....	12
4. Total RNA isolation and quantitative real-time PCR (Q-RT-PCR).....	12
5. Streptozotocin-induced diabetes mellitus mouse experiments.....	13
6. Statistical analysis .....	14
<b>III . Result</b> .....	<b>15</b>
1. IB-MECA promotes adipogenesis in hBM-MSCs. ....	15
2. Effect of IB-MECA on adipogenesis is independent of A <sub>3</sub> AR signaling..	19
3. Target deconvolution of IB-MECA and related A <sub>3</sub> AR ligands.....	25
4. IB-MECA and related A <sub>3</sub> AR ligands bind to PPAR $\gamma$ and PPAR $\delta$ . ....	28
5. IB-MECA and related A <sub>3</sub> AR ligands play roles as PPAR $\gamma$ partial agonists. .....	35

6. IB-MECA and related A <sub>3</sub> AR ligands play roles as PPAR $\delta$ antagonists....	37
7. Polypharmacophore in IB-MECA and related A <sub>3</sub> AR ligands improves insulin sensitivity in STZ-induced diabetic mice. ....	43
<b>IV. Discussion</b> .....	<b>46</b>
<b>V. Reference</b> .....	<b>51</b>
<b>요약 (국문초록)</b> .....	<b>58</b>

# LIST OF FIGURES

<b>Figure 1.</b> Chemical structures of adenosine, NECA, CCPA, CGS21680 and IB-MECA .....	16
<b>Figure 2.</b> Effects of AR signaling modulators on adipogenesis in hBM-MSCs .....	17
<b>Figure 3.</b> Structures of IB-MECA and related A <sub>3</sub> AR ligands and assessment of their adiponectin-promoting activity .....	21
<b>Figure 4.</b> Chemical structures of MRS5698 and MRE3008F20 and the assessment of their adiponectin-promoting activity .....	23
<b>Figure 5.</b> The pharmacological correlation between A <sub>3</sub> AR, A <sub>1</sub> AR, or A <sub>2A</sub> AR binding K <sub>i</sub> values and adiponectin levels of IB-MECA and related A <sub>3</sub> AR ligands .....	24
<b>Figure 6.</b> NRs competitive binding or coactivator activity and inhibitory activity on CDKs of IB-MECA and related A <sub>3</sub> AR ligands .....	26
<b>Figure 7.</b> TR-FRET PPAR $\alpha$ , PPAR $\gamma$ , and PPAR $\delta$ competitive binding assays with IB-MECA and related A <sub>3</sub> AR ligands .....	30
<b>Figure 8.</b> The pharmacological correlation between PPAR $\gamma$ or PPAR $\delta$ binding (%) and adiponectin levels of IB-MECA and related A <sub>3</sub> AR ligands .....	34
<b>Figure 9.</b> PPAR $\gamma$ transactivation activity of IB-MECA, Thio-IB-MECA, and compound <b>5</b> .....	36
<b>Figure 10.</b> PPAR $\delta$ coactivation and corepression activity of IB-MECA, Thio-IB-MECA and compound <b>5</b> .....	40

<b>Figure 11.</b> Transcriptional expression profile of ANGPTL4 and PDK4 during adipogenesis in hBM-MSCs .....	41
<b>Figure 12.</b> The adiponectin-promoting effects of PPAR $\delta$ antagonists in hBM-MSCs .....	42
<b>Figure 13.</b> Effects of IB-MECA, Thio-IB-MECA, and compound <b>5</b> on STZ-induced diabetic mice .....	44
<b>Figure 14.</b> The effects of compound <b>5</b> on serum glucose levels in STZ-induced diabetic mice .....	45



## LIST OF TABLES

<b>Table 1.</b> Binding affinities of IB-MECA and related A <sub>3</sub> AR ligands to human A <sub>1</sub> , A <sub>2A</sub> , and A <sub>3</sub> AR (19-21).....	22
<b>Table 2.</b> PPAR $\alpha$ binding activity of IB-MECA and related A <sub>3</sub> AR ligands.....	31
<b>Table 3.</b> PPAR $\gamma$ binding activity of IB-MECA and related A <sub>3</sub> AR ligands.....	32
<b>Table 3.</b> PPAR $\delta$ binding activity of IB-MECA and related A <sub>3</sub> AR ligands.....	33

# I . Introduction

Phenotype-based approaches has been suggested as an alternative to a defined target-based approaches in recent drug discovery (1, 2). For multifactorial metabolic diseases such as type II diabetes, obesity and osteoporosis, a phenotype-based assays have several advantages over target-based assays. The phenotypic assay based on the adipogenesis of human mesenchymal stem cells (hBM-MSCs) model was developed to study anti-diabetic and anti-obesity drugs (3, 4). Measuring adiponectin, an adipocytokine released from adipocytes, production and lipid accumulation can be diagnostic criteria for metabolic diseases (5, 6). In fact, sulfonylurea-type anti-diabetic drugs and peroxisome proliferator activated receptor (PPAR) $\gamma$  agonists increase adiponectin biosynthesis and lipid accumulation in hBM-MSCs model (3, 7). Non-steroidal anti-inflammatory drugs (NSAIDs) such as aspirin, ibuprofen, and indomethacin also increase adiponectin production during adipogenesis in hBM-MSCs, and ibuprofen and indomethacin bind to PPAR $\gamma$  at higher concentration (8, 9). However, aspirin does not bind to PPAR $\gamma$ , and the molecular targets associated with the effect is not fully understood. Our recent study demonstrated that monoamine oxidase inhibitors (MAOIs) such as moclobemide and Ro41-1049 significantly upregulated adiponectin production in hBM-MSCs, but the molecular targets are still unclear (10). Therefore, bioactive molecules discovered from phenotypic assays require additional study to identify and validate their direct molecular targets; this process is defined as drug target deconvolution (1, 2).

Adenosine receptors, G protein-coupled receptors (GPCR) consists of four subtypes: A<sub>1</sub>, A<sub>2A</sub>, A<sub>2B</sub>, and A<sub>3</sub> ARs. Extracellular adenosine plays a role in various physiological functions such as circulation, renal blood flow, cardiac rhythm, lipolysis, immune function, and angiogenesis. Notably, the regulation of ARs by agonists or antagonists has pharmacological significance in inflammatory diseases, neurodegenerative diseases, metabolic diseases, and cancers (11, 12).

Several reports indicate that ARs are associated with mammalian adipogenesis and osteogenesis. Caffeine, classified as a nonselective AR antagonist, is known for its inhibitory effects on adipogenesis in hMSCs (13, 14). Recent studies demonstrated the contrasting effects of A<sub>1</sub> and A<sub>2B</sub> AR on adipogenesis and the roles of adenosine on bone metabolism via A<sub>1</sub>, A<sub>2A</sub>, and A<sub>2B</sub> ARs in bone marrow cells (15, 16). In AR knockout mice, AR modulators showed potential anti-diabetic and anti-obesity activities (17). Also, in high-fat diet mice model, upregulated A<sub>2B</sub> AR was related with insulin receptor substrate 2 (IRS-2) expression, indicating the potential target for metabolic disease (18). Currently, the role of ARs in adipogenesis in hMSCs is not fully understood.

In this study, we evaluated the effect of various AR agonists and antagonists on adipogenesis in hBM-MSCs to elucidate specific roles of ARs. We discovered that a specific A<sub>3</sub> AR agonist N<sup>6</sup>-(3-iodobenzyl)adenosine-5'-N-methyluronamide (IB-MECA) and related A<sub>3</sub> AR ligands promoted adiponectin production during adipogenesis in hBM-MSCs. Unexpectedly, we found that most of A<sub>3</sub> AR antagonists, which are structurally similar to IB-MECA, also promoted adiponectin production in hBM-MSCs. In a target deconvolution study, we demonstrated the polypharmacological characteristic of IB-MECA and related A<sub>3</sub> AR ligands in

regulating adipogenesis in hBM-MSCs: A<sub>3</sub> AR modulator, a PPAR $\gamma$  partial agonist,  
and a PPAR $\delta$  antagonist.

## II. Materials and Methods

### 1. Cell culture and differentiation

hBM-MSCs were purchased from Lonza (Walkersville, MD, USA) and cultured as previously described (3, 4). To induce adipocyte differentiation, the growth medium was replaced by DMEM supplemented with 10% FBS, 10  $\mu\text{g/mL}$  insulin, 0.5  $\mu\text{M}$  dexamethasone, and 0.5 mM 3-isobutyl-1-methylxanthine (IBMX) (IDX condition). Dexamethasone, insulin, IBMX, glibenclamide, troglitazone, caffeine, NECA, CCPA, CGS21680, and T0901317 were purchased from Sigma–Aldrich (St. Louis, MO, USA). MRS5698, MRE3008F20, GW7647, GW1929, GW501516, GSK0660, and GSK3787 were purchased from Tocris Bioscience (Bristol, UK). IB-MECA, Cl-IB-MECA, Thio-IB-MECA, Thio-Cl-IB-MECA, and related  $A_3$  AR ligands, compounds **1** to **8**, were synthesized in house as previously reported (19–21). The level of adipocyte differentiation of hBM-MSCs was evaluated using an Oil Red O (ORO, Sigma-Aldrich) and hematoxylin (Sigma-Aldrich) staining method to measure intracellular lipid accumulation as previously reported (3, 4).

### 2. Enzyme-linked immunosorbent assay (ELISA)

For quantitative measurement of adiponectin in cell culture supernatants, a Quantikine™ immunoassay kit (R&D Systems, Minneapolis, MN, USA) was used,

and adiponectin concentrations were determined according to the manufacturer's instructions.

### **3. Nuclear receptor (NR) assays**

Time resolved fluorescence resonance energy transfer (TR-FRET)-based receptor binding assay was performed using Lanthascreen™ competitive binding assay kits (Invitrogen) to evaluate binding of ligands to NRs, PPAR $\alpha$ , PPAR $\gamma$ , PPAR $\delta$ , and GR. Lanthascreen™ coactivator assay kits were used to determine the ability to recruit coregulators of ligands to activate PPAR $\delta$ , LXR $\alpha$ , and LXR $\beta$ . We performed the Lanthascreen™ PPAR $\delta$  coactivator and corepressor assay using fluorescein-C33 coactivator peptide (Sequence: HVEMHPLLMGLLMESQWGA) and SMRT-ID2 peptide (Sequence: HASTNMGLEAHRKALMGKYDQW), respectively (22, 23). All assay measurements were performed using a CLARIOstar (BMG LABTECH, Ortenberg, Germany) according to the manufacturer's instructions. The luciferase reporter gene assay was performed as previously described (4).

### **4. Total RNA isolation and quantitative real-time PCR (Q-RT-PCR)**

Q-RT-PCR experiment was performed as previously reported (3, 4). TaqMan Universal Master Mix II and Q-RT-PCR primer sets (Applied Biosystems, Foster

City, CA, USA) were used according to the manufacturer's instructions to determine the transcription levels of adenosine A<sub>1</sub> AR (*ADORA1*, Hs00181231\_m1), A<sub>2A</sub> AR (*ADORA2A*, Hs00169123\_m1), A<sub>2B</sub> AR (*ADORA2B*, Hs00386497\_m1), A<sub>3</sub> AR (*ADORA3*, Hs00252933\_m1), angiotensin-like 4 (*ANGPTL4*, Hs01101127\_m1), and pyruvate dehydrogenase kinase, isozyme 4 (*PDK4*, Hs01037712\_m1). Human glyceraldehyde-3-phosphate dehydrogenase (*GAPDH*, 4333764F) was used to normalize sample variations. Q-RT-PCR was performed with an Applied Biosystems 7500 Real-Time PCR System (Applied Biosystems). Relative gene expression levels were quantified using equations from a mathematical model developed by Pfaffl (24).

## **5. Streptozotocin-induced diabetes mellitus mice experiments**

A single dose of 180 mg/kg of streptozotocin (STZ) was intraperitoneally administered to 5-week old C57BL/6J mice. From the 7<sup>th</sup> day after the STZ treatment, serum glucose concentration was monitored daily for three consecutive days after 2 hours of fasting. The glucose concentration was measured with a portable glucose meter Accu-Check Active (Boehringer-Mannheim Biochemicals, Indianapolis, IN, USA). Mice with a serum glucose concentration higher than 300 mg/dl were considered diabetic. Before administration of drugs, serum glucose concentration was confirmed again at 2 hours after fasting and potential anti-diabetic drugs were orally administered daily for 5 days. On the 5<sup>th</sup> day, serum glucose levels were measured just before drug administration (0 hour) and 1 and 4

hours after drug administration. Blood samples were obtained from the tail vein with heparinized syringes. Serum triglycerides were determined with a Serum Triglyceride Determination Kit (TR0100, Sigma-Aldrich) and lactate levels were quantified with a Lactate Assay Kit (MAK064, Sigma-Aldrich).

## **6. Statistical analysis**

Statistical analysis was conducted using RStudio<sup>®</sup> for Windows (RStudio Inc., Boston, MA, USA). Experimental values are expressed as the means  $\pm$  standard deviation (SD) from three or four independent experiments. Statistical analysis was performed using one-way analysis of variance (ANOVA) and post-hoc tests. Correlation coefficient was also calculated by RStudio<sup>®</sup> for Windows.



### III. Results

#### 1. IB-MECA promotes adipogenesis in hBM-MSCs.

In the hBM-MSC-based phenotypic assay, various AR agonists were tested whether AR signaling affects adipogenesis in hBM-MSCs. An endogenous ligand adenosine, a nonselective AR agonist NECA, A<sub>1</sub> AR agonist CCPA, A<sub>2A</sub> AR agonist CGS21680, or A<sub>3</sub> AR agonist IB-MECA, or a non-specific AR antagonist caffeine were added to the cells along with the IDX adipogenesis-inducing medium (Fig. 1). After 7 days in culture, the supernatants of cells were harvested and adiponectin ELISA was performed (Fig. 2). Compared to the level of adiponectin, in the IDX control, that in adenosine-, CCPA-, NECA-, or CGS21680-treated cells did not significantly promote adiponectin production during adipogenesis in hBM-MSCs (Fig. 2A). A known inhibitory agent, caffeine significantly inhibited adipogenesis in hBM-MSCs, and which was proven through ORO staining (Fig 2A, B). Only the A<sub>3</sub> AR agonist IB-MECA significantly promoted adiponectin production during adipogenesis in hBM-MSCs in a concentration-dependent manner (Fig. 2C). In addition, the increased lipid droplet stained with ORO demonstrated that IB-MECA promotes differentiation to adipocyte in hBM-MSCs comparing to IDX control (Fig. 2B).

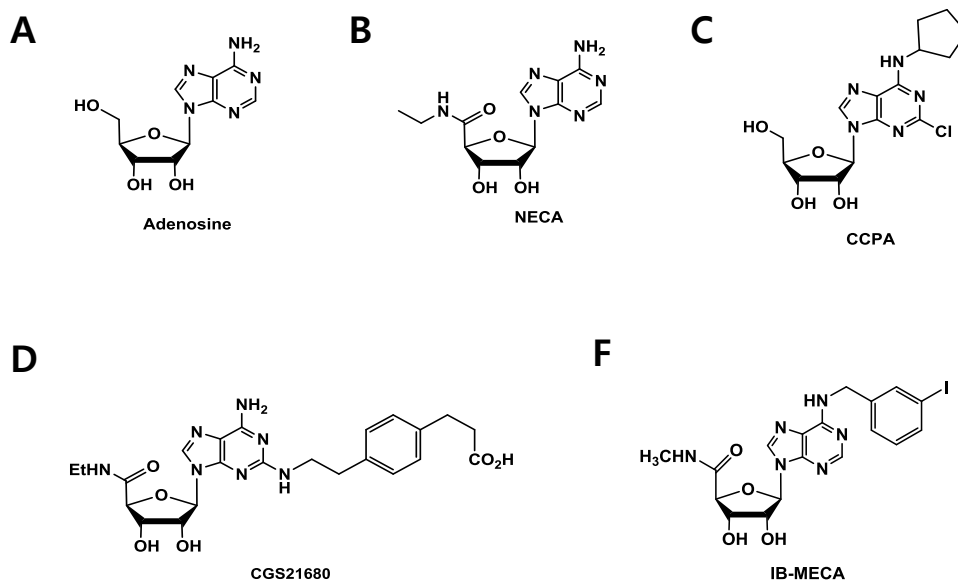
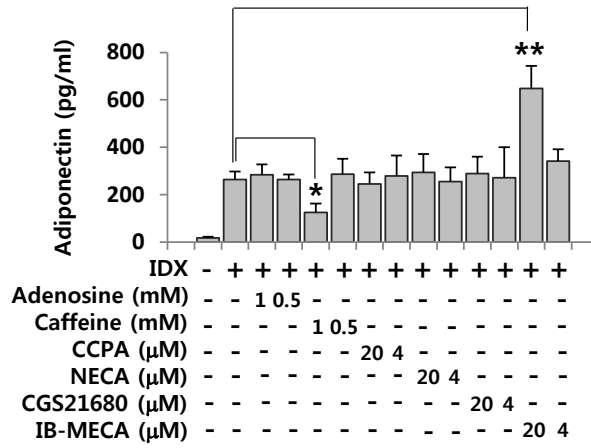


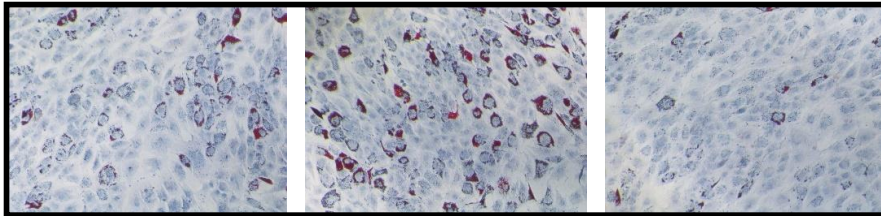
**Figure 1. Chemical structures of adenosine, NECA, CCPA, CGS21680 and IB-MECA**

Chemical structures of an endogenous ligand adenosine (A), a nonselective AR agonist NECA (B), A<sub>1</sub> AR agonist CCPA (C), A<sub>2A</sub> AR agonist CGS21680 (D), and A<sub>3</sub> AR agonist IB-MECA (F) were drawn with ChemBioDraw Ultra<sup>®</sup> (Perkinelmer, Waltham, MA, USA).

**A**



**B**



Insulin + Dexamethasone + IDX + IB-MECA 20 μM    Insulin + Dexamethasone + IDX + Caffeine 1 mM  
 Insulin + Dexamethasone + IBMX (IDX)

**C**

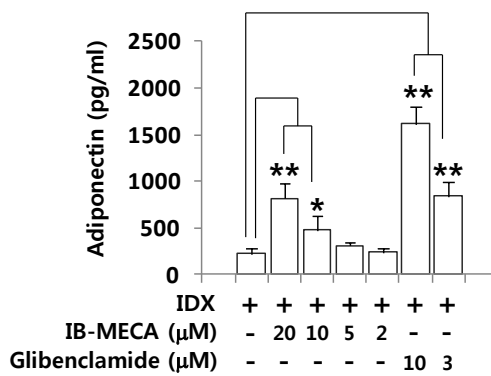


**Figure 2. Effects of AR signaling modulators on adipogenesis in hBM-MSCs**

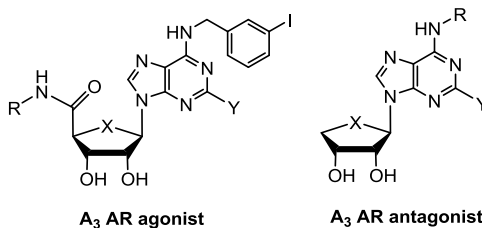
(A) hBM-MSCs were grown under IDX conditions and/or co-treated with adenosine, caffeine, CCPA, NECA, CGS21680, or IB-MECA. On the 7th day in culture, the supernatant was harvested and ELISA was performed to measure the levels of adiponectin accumulated in the supernatants over 48 hours. (B) ORO staining was performed to estimate lipid droplets on the 7th day in culture. (C) The levels of adiponectin in the supernatants of IB-MECA-treated cells were evaluated in a concentration-dependent manner. Results are the mean  $\pm$  SD of three measurements using hBM-MSCs from three independent donors ( $n = 3$ ). \*  $p \leq 0.05$  and \*\*  $p \leq 0.01$ .

## 2. Effect of IB-MECA on adipogenesis is independent of A<sub>3</sub> AR signaling.

In the previous research, we have reported the results of structure-activity studies on novel A<sub>3</sub> AR agonists and antagonists, whose pharmacophore was structurally related to IB-MECA (Fig. 3, Table 1) (19-21). In order to figure out the association of A<sub>3</sub> AR signaling pathway with the regulation of adipogenesis in hBM-MSCs, we evaluated the effects of synthesized A<sub>3</sub> AR agonists and antagonists on adiponectin production (Fig. 3). IB-MECA, Cl-IB-MECA, Thio-IB-MECA, and other A<sub>3</sub> AR agonists, compounds **1-4** significantly promoted adiponectin production in hBM-MSCs (Fig. 3). Surprisingly, A<sub>3</sub> AR antagonists, compound **5-8**, also increased the adiponectin production in the same assay (Fig. 3). The most potent compound to promote adipogenesis in hBM-MSCs was compound **5** at a concentration of 20 μM among them (Fig. 3). These results suggests that A<sub>3</sub> AR signaling is not associated with adiponectin-promoting activity during adipogenesis in hBM-MSCs. To address this question, we investigated the effects of A<sub>3</sub> AR ligands MRS5698 and MRE3008F20 which are structurally different from IB-MECA, on the production of adiponectin in hBM-MSCs (Fig. 4). Unlike IB-MECA and related A<sub>3</sub> AR ligands, A<sub>3</sub> AR agonist and antagonist, MRS5698 and MRE3008F20 had no effects on adipogenesis in hBM-MSCs (Fig. 4). To confirm the independence of A<sub>3</sub> AR binding affinity and adiponectin-promoting activity of IB-MECA and related A<sub>3</sub> AR ligands, we calculated the correlation (Fig. 3, 5A, Table1). The correlation coefficient ( $r^2$ ) between the adiponectin-promoting activity at 20 μM and  $K_i$  values of the IB-MECA-related A<sub>3</sub> AR ligands was 0.04 ( $p = 0.54$ ), which indicates no

statistically significant association between the two variables (Fig. 5A). When comparing the A<sub>1</sub> or A<sub>2A</sub> AR binding affinity of these compounds, no significant correlation was observed (Fig. 5B, C). Taken together, these results suggest that the effect of IB-MECA and related A<sub>3</sub> AR ligands on adipogenesis in hBM-MSCs was independent of the A<sub>3</sub> AR signaling pathway.

**A**



	X	Y	R	Adiponectin (pg/ml)		
				20 $\mu$ M	4 $\mu$ M	
A <sub>3</sub> AR agonist	IB-MECA	O	H	CH <sub>3</sub>	216 $\pm$ 12**	117 $\pm$ 20
	Cl-IB-MECA	O	Cl	CH <sub>3</sub>	603 $\pm$ 10**	221 $\pm$ 10**
	Thio-IB-MECA	S	H	CH <sub>3</sub>	343 $\pm$ 20**	126 $\pm$ 14
	Thio-Cl-IB-MECA	S	Cl	CH <sub>3</sub>	738 $\pm$ 59**	131 $\pm$ 10
	Compound 1	S	H	CH <sub>2</sub> CH <sub>3</sub>	242 $\pm$ 4**	118 $\pm$ 38
	Compound 2	S	H	Cyclopropyl	249 $\pm$ 26**	174 $\pm$ 5**
	Compound 3	S	H	Cyclopropyl-CH <sub>2</sub>	490 $\pm$ 16**	242 $\pm$ 11**
	Compound 4	S	H	Cyclobutyl	633 $\pm$ 39**	323 $\pm$ 30**
A <sub>3</sub> AR antagonist	Compound 5	S	Cl	3-I-Bn	857 $\pm$ 69**	192 $\pm$ 19*
	Compound 6	S	Cl	3-Cl-Bn	442 $\pm$ 5**	196 $\pm$ 1**
	Compound 7	S	Cl	2-Cl-Bn	268 $\pm$ 14**	107 $\pm$ 6
	Compound 8	S	H	3-Cl-Bn	247 $\pm$ 7**	163 $\pm$ 12*
IDX control					100 $\pm$ 6	
Glibenclamide					1000 $\pm$ 193**	838 $\pm$ 67**

**B**

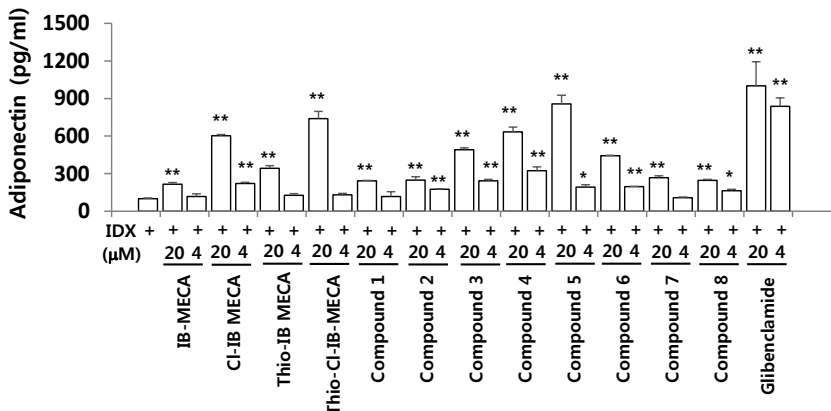


**Figure 3. Structures of IB-MECA and related A<sub>3</sub> AR ligands and assessment of their adiponectin-promoting activity**

IB-MECA and related A<sub>3</sub> AR ligands (A) were co-treated with the IDX adipogenesis-inducing medium as described in the materials and methods. On the 7th day in culture, cell culture supernatants were harvested and ELISA was performed to measure levels of adiponectin (A, B). Values represent mean  $\pm$  SD (n = 3). \*  $p \leq 0.05$  and \*\*  $p \leq 0.01$ .

		$K_i$ (hA <sub>1</sub> AR) nM or % displ. at 1 $\mu$ M	$K_i$ (hA <sub>2A</sub> AR) nM or % displ. at 1 $\mu$ M	$K_i$ (hA <sub>3</sub> AR) nM or % displ. at 1 $\mu$ M
A <sub>3</sub> AR agonist	IB-MECA	51.2 $\pm$ 5.1	2910 $\pm$ 580	1.8 $\pm$ 0.7
	Cl-IB-MECA	222 $\pm$ 22	5360 $\pm$ 2470	1.4 $\pm$ 0.3
	Thio-IB-MECA	20.2 $\pm$ 2.9	475 $\pm$ 144	0.3 $\pm$ 0.1
	Thio-Cl-IB-MECA	193 $\pm$ 46	223 $\pm$ 36	0.38 $\pm$ 0.07
	Compound 1	5.4 $\pm$ 0.3	57.6 $\pm$ 6.9	0.42 $\pm$ 0.22
	Compound 2	9.27 $\pm$ 0.83	15.2 $\pm$ 2.6	3.03 $\pm$ 0.23
	Compound 3	159 $\pm$ 40	1600 $\pm$ 80	2.16 $\pm$ 0.29
	Compound 4	23.6 $\pm$ 4.2	122 $\pm$ 62	1.17 $\pm$ 0.16
A <sub>3</sub> AR antagonist	Compound 5	2490 $\pm$ 940	341 $\pm$ 75	4.16 $\pm$ 0.5
	Compound 6	38%	18%	1.66 $\pm$ 0.9
	Compound 7	13%	1600 $\pm$ 135	25.8 $\pm$ 6.3
	Compound 8	860 $\pm$ 210	440 $\pm$ 110	1.5 $\pm$ 0.4

**Table 1. Binding affinities of IB-MECA and related A<sub>3</sub> AR ligands to human A<sub>1</sub>, A<sub>2A</sub>, and A<sub>3</sub> AR (19-21)**

All AR experiments were performed using adherent Chinese hamster ovary (CHO) cells stably transfected with cDNA encoding the human ARs as previously described. A<sub>3</sub> AR binding  $K_i$  value and percent displacement of the human A<sub>3</sub> AR were determined at 1  $\mu$ M. Binding to the human ARs was carried out using the radioligands [3H]R-PIA for A<sub>1</sub> AR, [3H]CGS21680 for A<sub>2A</sub> AR, and [125I]I-AB-MECA for A<sub>3</sub> AR. Values from the present study are expressed as means  $\pm$  standard error of the mean (SEM) (n = 3–5).



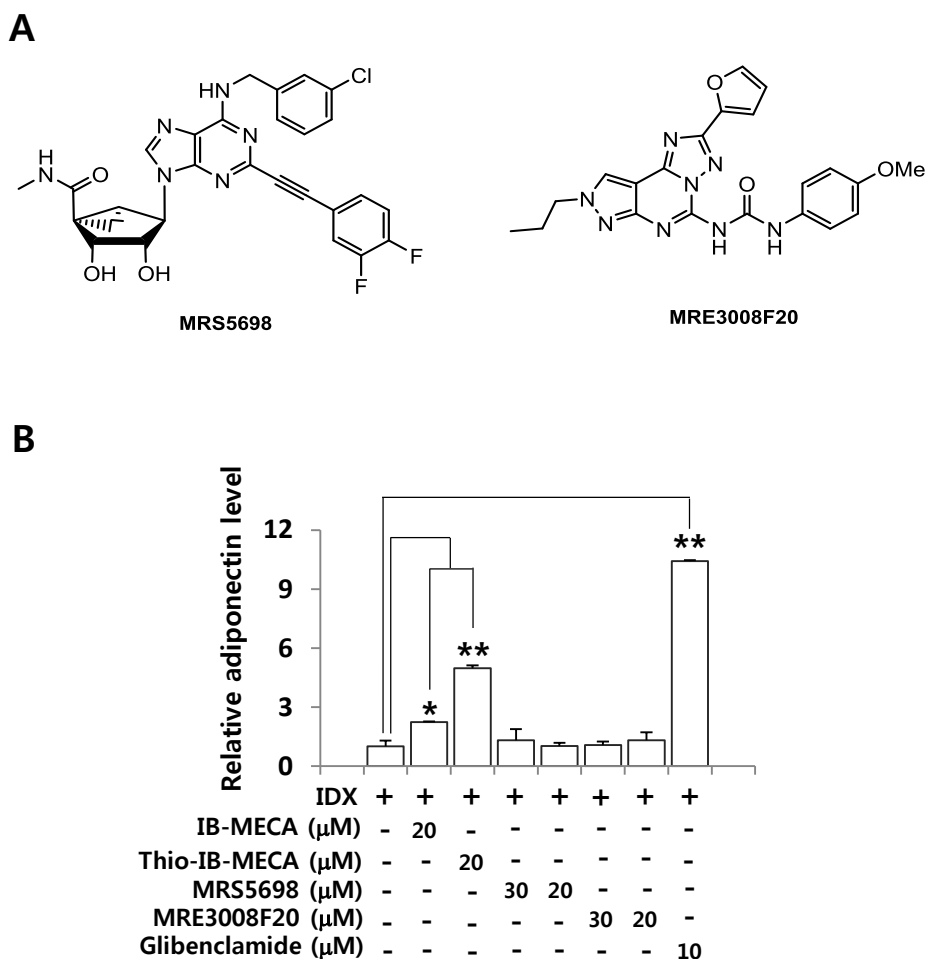


**Figure 4. Chemical structures of MRS5698 and MRE3008F20 and the assessment of their adiponectin-promoting activity**

The effects of A<sub>3</sub> AR agonists IB-MECA, Thio-IB-MECA and chemically different agonist MRS5698 (A), and antagonist MRE3008F20 (A) on adiponectin production in hBM-MSCs during adipogenesis were evaluated (B). Values represent mean ± SD (n = 3). \*  $p \leq 0.05$  and \*\*  $p \leq 0.01$ .

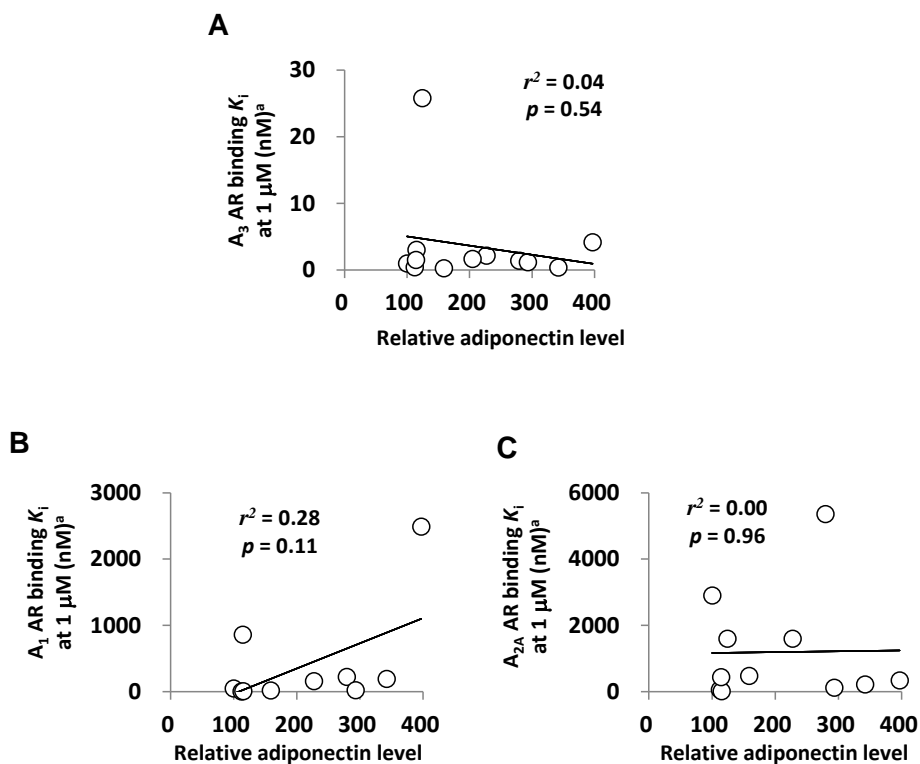


**Figure 5. The pharmacological correlation between  $A_3$  AR,  $A_1$  AR, or  $A_{2A}$  AR binding  $K_i$  values and adiponectin levels of IB-MECA and related  $A_3$  AR ligands.**

The correlation coefficient was calculated between  $A_3$  AR (A),  $A_1$  AR (B), or  $A_{2A}$  AR (C) binding  $K_i$  values at 1  $\mu$ M and adiponectin levels at 20  $\mu$ M of IB-MECA and related  $A_3$  AR ligands. Values represent mean  $\pm$  SD (n = 3).

### **3. Target deconvolution of IB-MECA and related A<sub>3</sub> AR ligands.**

For the target deconvolution, TR-FRET NRs competitive binding and coactivator assays were performed (Fig. 6A). NRs such as PPAR $\alpha$ , PPAR $\gamma$ , PPAR $\delta$ , liver X receptor (LXR) $\alpha$ , LXR $\beta$ , and glucocorticoid receptor (GR) play roles in mammalian adipogenesis (25). The result indicated that IB-MECA and Cl-IB-MECA significantly binds to PPAR $\gamma$  and PPAR $\delta$  (Fig. 6A). In the TR-FRET receptor binding assay, 4  $\mu$ M IB-MECA and Cl-IB-MECA competitively inhibited the binding of the labeled PPAR $\delta$  ligand by 26% and 75%, respectively. The binding of labeled PPAR $\gamma$  ligand was also inhibited by Cl-IB-MECA by 59%. No significant effect on PPAR $\alpha$ , LXR $\alpha$ , LXR $\beta$ , or GR was observed (Fig. 6A). Recently, cyclin-dependent kinase 5 (CDK5) was reported to regulate adipogenesis by affecting PPAR $\gamma$  phosphorylation (26). Therefore, we also evaluated the inhibitory effects of IB-MECA and Cl-IB-MECA on CDK5 activity. At concentrations up to 10  $\mu$ M, neither IB-MECA nor Cl-IB-MECA affected CDKs activity (Fig. 6B).

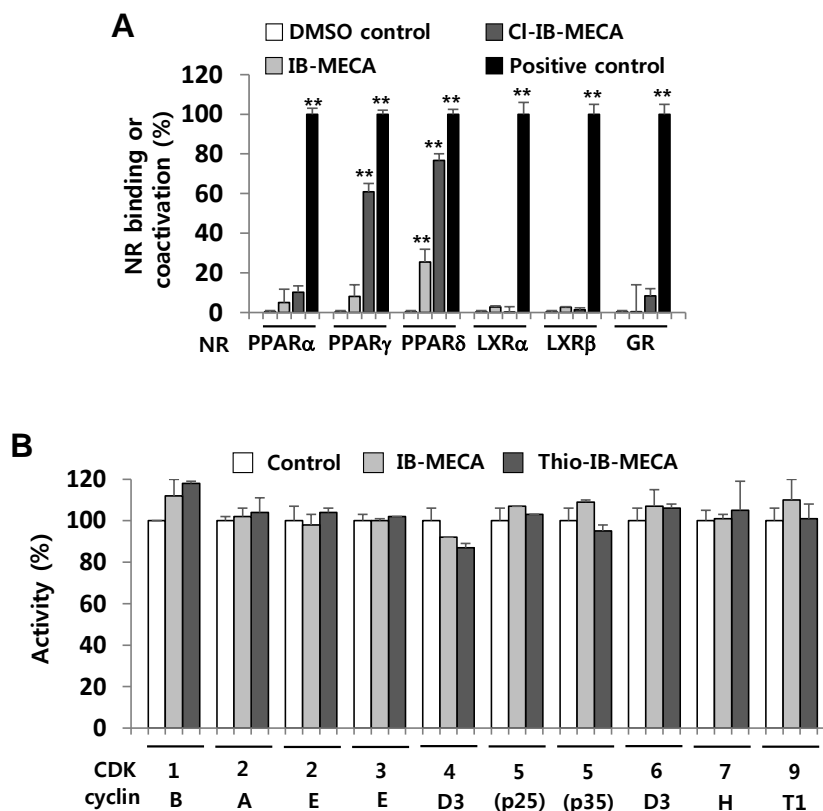


**Figure 6. NRs competitive binding or coactivator activity and inhibitory activity on CDKs of IB-MECA and related A<sub>3</sub> AR ligands**

(A) TR-FRET competitive binding assays (PPAR $\alpha$ , PPAR $\gamma$ , PPAR $\delta$ , and GR) and coactivator assays (LXR $\alpha$  and LXR $\beta$ ) with IB-MECA and Cl-IB-MECA at 4  $\mu$ M were performed. The positive controls included GW7647 for PPAR $\alpha$ , GW1929 for PPAR $\gamma$ , GW501516 for PPAR $\delta$ , dexamethasone for GR, and T0901317 for LXR $\alpha$  and LXR $\beta$ . DMSO in buffer was used as a blank control. (B) The kinase inhibitor assay using KinaseProfiler<sup>TM</sup> (Eurofins, Dundee, UK) was carried out. The inhibitory effects of IB-MECA and Thio-IB-MECA at 4  $\mu$ M on the phosphorylation of CDK1/cyclin B, CDK2/cyclin A, CDK2/cyclin E, CDK3/cyclin

E, CDK4/cyclin D3, CDK5/p25, CDK5/p35, CDK6/cyclin D3, CDK7/cyclin H, and CDK/cyclin T1 were tested at each  $K_m$  ATP concentration. DMSO was included in each negative control. Values were expressed in terms of percentage compared to each positive control (n = 2, 3). \*  $p \leq 0.05$  and \*\*  $p \leq 0.01$ .

## 4. IB-MECA and related A<sub>3</sub> AR ligands bind to PPAR $\gamma$ and PPAR $\delta$ .

We determined the concentration–response relationship of IB-MECA and related A<sub>3</sub> AR ligands in terms of their binding activity to PPAR $\alpha$ , PPAR $\gamma$ , and PPAR $\delta$  (Fig. 7, Table 2-4). In the PPAR $\alpha$  binding assay, up to 20  $\mu$ M of IB-MECA and related A<sub>3</sub> AR ligands did not significantly displace >50% of the labeled PPAR $\alpha$  ligand (Fig. 7A, Table 2). In the PPAR $\gamma$  analysis, Cl-IB-MECA, Thio-IB-MECA, and compound **5** displayed significant competitive binding activity in a concentration-dependent manner (Fig. 7B, Table 3). The  $K_i$  values of Cl-IB-MECA, Thio-IB-MECA, and compound **5** were 0.472, 2.445, and 0.005, respectively, but not as potent as the PPAR $\gamma$  agonist GW1929 (Fig. 7B). Consistent with the literature (7), glibenclamide, a sulfonylurea antidiabetic drug, directly bound to PPAR $\gamma$  ligand-binding domain in the TR-FRET-based assay (Fig. 7B). Compared to PPAR $\alpha$  and PPAR $\gamma$  binding activities, IB-MECA and most related A<sub>3</sub> AR ligands notably displaced the labeled PPAR $\delta$  ligand in a concentration-dependent manner (Fig. 7C, Table 4). Importantly, compounds **5** and **6** exhibited maximal PPAR $\delta$  binding activity compared to that of a PPAR $\delta$  agonist GW501516 (Fig. 7C). The  $K_i$  values for PPAR $\delta$  binding of compounds **5** and **6**, which were characterized as A<sub>3</sub> AR antagonists, were 5 and 10 nM, respectively (Fig. 7C, Table 4). Surprisingly, a significant correlation was observed between the level of PPAR $\gamma$  ligand binding at 20 and 4  $\mu$ M and the adiponectin-promoting activity in hBM-MSCs (Fig. 8A, B). The correlation coefficient ( $r^2$ ) at 20  $\mu$ M and 4  $\mu$ M was

0.57 ( $p < 0.01$ ) and 0.43 ( $p < 0.05$ ), respectively. At lower concentration 2 and 0.4  $\mu\text{M}$ , the significant associations were observed between PPAR $\delta$  binding affinity and adiponectin-promoting activity (Fig. 8C, D). The value of the correlation coefficient ( $r^2$ ) at 2  $\mu\text{M}$  and 0.4  $\mu\text{M}$  was 0.52 ( $p < 0.01$ ) and 0.78 ( $p < 0.01$ ), respectively. As a result, the effects of IB-MECA and related A<sub>3</sub> AR ligands on PPAR $\delta$  occurred at lower concentrations than those for PPAR $\gamma$  in terms of adipogenesis-inducing activity. Taken together, IB-MECA and related A<sub>3</sub> AR ligands promote adiponectin production in hBM-MSCs by modulating the activity of PPAR $\gamma$  and PPAR $\delta$ , not A<sub>3</sub> AR.

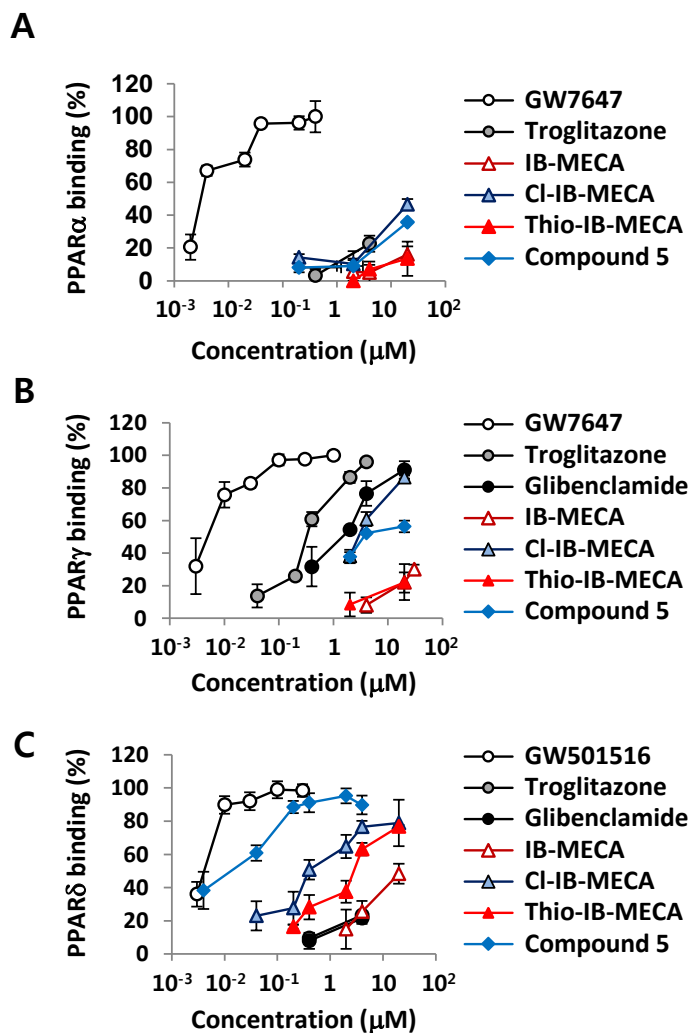


**Figure 7. TR-FRET PPAR $\alpha$ , PPAR $\gamma$ , and PPAR $\delta$  competitive binding assays with IB-MECA and related A<sub>3</sub> AR ligands**

The competitive binding activities of troglitazone, IB-MECA, CI-IB-MECA, Thio-IB-MECA, and compound 5 to PPAR $\alpha$ , PPAR $\gamma$ , and PPAR $\delta$  (A-C) and glibenclamide to PPAR $\gamma$ , and PPAR $\delta$  (B and C) were evaluated. Percentage values represent mean  $\pm$  SD (n = 3).



**Table 2. PPAR $\alpha$  binding activity of IB-MECA and related A<sub>3</sub> AR ligands**

		PPAR $\alpha$ (% replacement) <sup>a</sup>	
		20 $\mu$ M	4 $\mu$ M
A <sub>3</sub> AR agonist	IB-MECA	16.0 $\pm$ 4.9**	5.02 $\pm$ 6.77
	CI-IB-MECA	46.5 $\pm$ 3.3**	10.2 $\pm$ 3.3
	Thio-IB-MECA	13.5 $\pm$ 10.4**	6.90 $\pm$ 2.73**
	Thio-CI-IB-MECA	37.8 $\pm$ 2.3**	37.5 $\pm$ 6.3**
	Compound 1	29.3 $\pm$ 8.3**	16.9 $\pm$ 7.6*
	Compound 2	37.6 $\pm$ 5.2**	26.8 $\pm$ 7.0**
	Compound 3	16.4 $\pm$ 3.0**	8.90 $\pm$ 2.08**
	Compound 4	11.7 $\pm$ 2.0*	19.8 $\pm$ 9.5*
A <sub>3</sub> AR antagonist	Compound 5	35.6 $\pm$ 0.6**	9.03 $\pm$ 9.09
	Compound 6	4.50 $\pm$ 4.61	8.50 $\pm$ 5.9
	Compound 7	19.2 $\pm$ 2.4**	20.6 $\pm$ 11.6*
	Compound 8	18.5 $\pm$ 3.6**	12.4 $\pm$ 4.4*

<sup>a</sup> TR-FRET competitive ligand binding activity of IB-MECA and related A<sub>3</sub> AR ligands was evaluated (22-24). The potent compounds displaced the fluorescent ligands from the recombinant GST-PPAR ligand-binding domain (LBD). Results are expressed as the percentage of displacement calculated from the ratio of fluorescence intensity at 520 nm and 495 nm. The  $K_i$  of the positive control GW7647 was 0.0541  $\pm$  0.0089 in the parallel study. Values represent the mean expression  $\pm$  SD (n = 3). \*  $p \leq 0.05$  and \*\*  $p \leq 0.01$ .

**Table 3. PPAR $\gamma$  binding activity of IB-MECA and related A $_3$  AR ligands**

		PPAR $\gamma$ (% replacement) <sup>b</sup>			K $_i$ <sup>a</sup>
		20 $\mu$ M	4 $\mu$ M	2 $\mu$ M	
A $_3$ AR agonist	IB-MECA	22.2 $\pm$ 7.3*	8.10 $\pm$ 3.34	2.30 $\pm$ 4.75	ND
	CI-IB-MECA	86.6 $\pm$ 1.0**	60.9 $\pm$ 4.2**	38.2 $\pm$ 2.3**	2.18 $\pm$ 0.32
	Thio-IB-MECA	46.9 $\pm$ 6.2**	26.3 $\pm$ 7.3*	39.3 $\pm$ 3.5**	ND
	Thio-CI-IB-MECA	75.7 $\pm$ 1.5**	34.9 $\pm$ 4.9**	13.6 $\pm$ 2.1*	4.60 $\pm$ 0.26
	Compound 1	37.1 $\pm$ 3.7**	37.4 $\pm$ 8.7**	37.0 $\pm$ 2.2**	ND
	Compound 2	49.1 $\pm$ 6.1**	36.6 $\pm$ 10.1**	31.4 $\pm$ 6.4*	ND
	Compound 3	67.8 $\pm$ 3.3**	51.2 $\pm$ 3.9**	44.3 $\pm$ 2.8**	1.83 $\pm$ 0.25
	Compound 4	84.5 $\pm$ 2.7**	73.5 $\pm$ 7.9**	48.8 $\pm$ 6.3**	0.172 $\pm$ 0.063
A $_3$ AR antagonist	Compound 5	56.4 $\pm$ 3.6**	52.3 $\pm$ 0.8**	37.9 $\pm$ 4.1**	3.42 $\pm$ 0.47
	Compound 6	40.8 $\pm$ 2.8**	24.3 $\pm$ 5.7*	31.1 $\pm$ 3.0*	ND
	Compound 7	30.3 $\pm$ 4.8*	28.2 $\pm$ 15.6	24.0 $\pm$ 15.6	ND
	Compound 8	32.1 $\pm$ 10.7*	22.8 $\pm$ 7.2*	27.3 $\pm$ 3.9*	ND

<sup>a</sup> The K $_i$  of the positive control GW1929 in the parallel experiment was 0.0497  $\pm$  0.0115. Troglitazone and glibenclamide showed 96.2% and 77.5% binding to PPAR $\gamma$  at 10  $\mu$ M respectively. Values represent the mean expression  $\pm$  SD (n = 3). \*  $p \leq 0.05$  and \*\*  $p \leq 0.01$ . <sup>b</sup> ND : not determined.

**Table 4. PPAR $\delta$  binding activity of IB-MECA and related A $_3$  AR ligands**

		PPAR $\delta$ (% replacement) <sup>b</sup>					K $_i$ <sup>a</sup>
		20 $\mu$ M	4 $\mu$ M	2 $\mu$ M	0.2 $\mu$ M	0.02 $\mu$ M	
A $_3$ AR agonist	IB-MECA	48.3 $\pm$ 6.0**	25.5 $\pm$ 6.4*	15.0 $\pm$ 11.9	ND	ND	ND
	Cl-IB-MECA	78.9 $\pm$ 14.0**	76.7 $\pm$ 3.5**	64.8 $\pm$ 7.0**	27.7 $\pm$ 9.9*	ND	0.432 $\pm$ 0.033
	Thio-IB-MECA	76.9 $\pm$ 0.8**	63.2 $\pm$ 3.8**	33.1 $\pm$ 6.6**	ND	ND	2.54 $\pm$ 0.15
	Thio-Cl-IB-MECA	ND	92.0 $\pm$ 3.9**	77.2 $\pm$ 20.4**	45.5 $\pm$ 34.4**	ND	0.160 $\pm$ 0.092
	Compound 1	71.9 $\pm$ 5.2**	53.7 $\pm$ 4.0**	32.1 $\pm$ 6.9*	ND	ND	3.15 $\pm$ 0.47
	Compound 2	71.6 $\pm$ 6.5**	61.1 $\pm$ 6.6**	38.8 $\pm$ 9.8**	ND	ND	2.988 $\pm$ 0.397
	Compound 3	81.5 $\pm$ 2.0**	59.9 $\pm$ 7.6**	32.7 $\pm$ 6.4**	ND	ND	2.373 $\pm$ 0.668
	Compound 4	75.2 $\pm$ 3.1**	47.4 $\pm$ 9.9**	40.8 $\pm$ 6.9**	ND	ND	2.612 $\pm$ 0.721
A $_3$ AR antagonist	Compound 5	ND	89.7 $\pm$ 5.7**	91.6 $\pm$ 4.5**	88.5 $\pm$ 3.6**	38.3 $\pm$ 11.2**	0.00483 $\pm$ 0.0023
	Compound 6	ND	93.1 $\pm$ 3.8**	87.5 $\pm$ 5.2**	70.8 $\pm$ 4.8**	27.8 $\pm$ 7.2*	0.0102 $\pm$ 0.0910
	Compound 7	79.3 $\pm$ 8.1**	61.4 $\pm$ 1.7**	40.4 $\pm$ 0.5**	10.7 $\pm$ 18.3	ND	0.620 $\pm$ 0.654
	Compound 8	49.1 $\pm$ 5.2**	13.1 $\pm$ 8.2	30.3 $\pm$ 6.0*	ND	ND	ND

<sup>a</sup> The K $_i$  of the positive control GW501516 was 0.0480  $\pm$  0.0014 in the parallel experiment. Troglitazone and glibenclamide bound to PPAR $\delta$  23.4% and 21.5% at 10  $\mu$ M respectively, compared to GW501516. Values represent the mean expression  $\pm$  SD (n = 3). \*  $\leq$  0.05 and \*\*  $p \leq$  0.01. <sup>b</sup> ND : not determined.

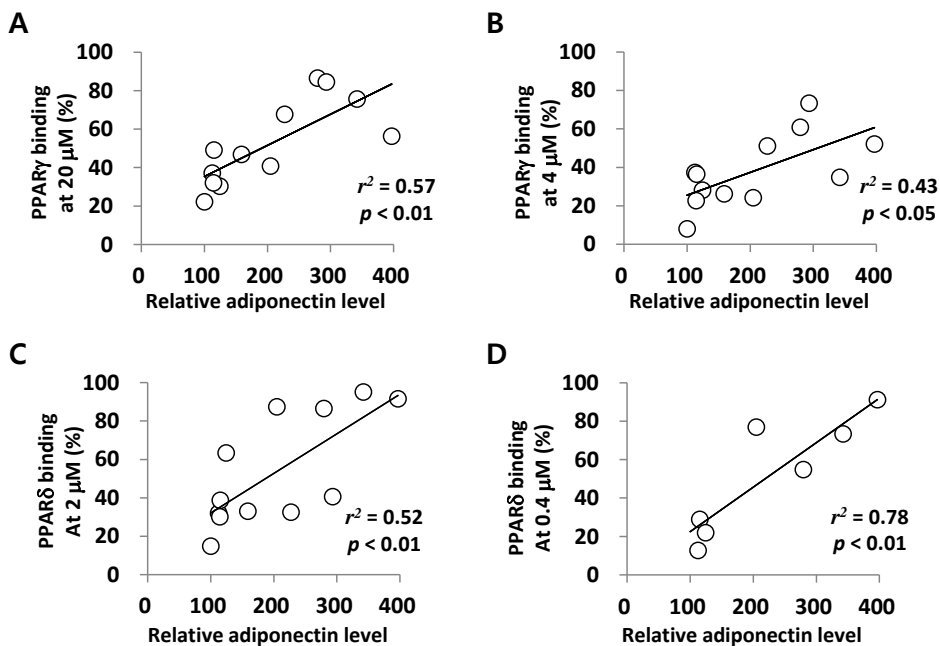


**Figure 8. The pharmacological correlation between PPAR $\gamma$  or PPAR $\delta$  binding (%) and adiponectin levels of IB-MECA and related A<sub>3</sub> AR ligands**

The correlation coefficient was calculated between PPAR $\gamma$  at 20  $\mu$ M (A) and 4  $\mu$ M (B), and PPAR $\delta$  at 2  $\mu$ M (C) and 0.4  $\mu$ M (D) and relative adiponectin levels at 20  $\mu$ M of IB-MECA and related A<sub>3</sub> AR ligands. Correlation coefficient ( $r^2$ ) was calculated with RStudio<sup>®</sup> software.

## **5. IB-MECA and related A<sub>3</sub> AR ligands play roles as PPAR $\gamma$ partial agonists.**

Based on the fact that PPAR $\gamma$  agonists promote adipogenesis in hBM-MSCs, we investigated whether IB-MECA and related A<sub>3</sub> AR ligands are PPAR $\gamma$  agonists or not. To determine a functional outcome for the effect of IB-MECA, Thio-IB-MECA, and compound **5** on PPAR $\gamma$ , we performed a luciferase-reporter PPAR $\gamma$  transactivation assay (4). At 10  $\mu$ M, IB-MECA, Thio-IB-MECA, and compound **5** increased PPAR $\gamma$  transactivation by 29.9%, 46.9%, and 54.3%, respectively (Fig. 9). The most potent agent, compound **5** (30  $\mu$ M) did not achieve maximal PPAR $\gamma$  transactivation activity compared to troglitazone, a PPAR $\gamma$  full agonist; this result corresponded to that of a PPAR $\gamma$  binding assay (Fig. 7B). In conclusion, PPAR $\gamma$  partial agonism may contribute to the adiponectin-promoting activity of IB-MECA and related A<sub>3</sub> AR ligands.

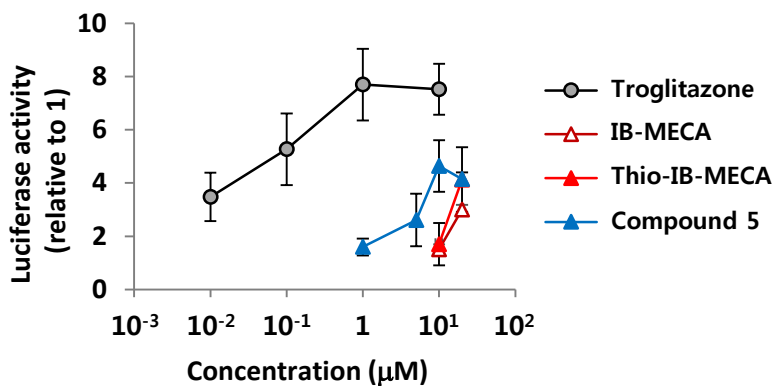


**Figure 9. PPAR $\gamma$  transactivation activity of IB-MECA, Thio-IB-MECA, and compound 5**

CV-1 cells were transiently cotransfected with the PPAR $\gamma$  expression vector and the PPAR $\gamma$  responsive elements (PPRE)-luciferase reporter, and then treated with troglitazone, IB-MECA, Thio-IB-MECA, or compound 5. Results are the mean  $\pm$  SD of three measurements using independent hBM-MSCs (n = 3).

## **6. IB-MECA and related A<sub>3</sub> AR ligands play roles as PPAR $\delta$ antagonists.**

To elucidate a functional consequence for PPAR $\delta$ , we performed a TR-FRET PPAR $\delta$  coactivator assay, which measures the level of interaction between the PPAR $\delta$  ligand-binding domain and a fluorescein-labeled coactivator peptide. GW501516, a selective PPAR $\delta$  agonist, increased the fluorescence signal by the recruitment of peptides in the TR-FRET assay system in a concentration-dependent manner (Fig. 10A). IB-MECA, Thio-IB-MECA, compound **5**, and a PPAR $\delta$  antagonist, GSK0660 had no effect on the transactivation. To confirm the PPAR $\delta$  antagonism, we evaluated whether IB-MECA, Thio-IB-MECA, and compound **5** competitively inhibit the GW501516-induced coactivator recruitment to PPAR $\delta$  (Fig. 10B). Compound **5** (1  $\mu$ M) significantly decreased the recruitment effect of GW501516 on PPAR $\delta$  coactivator by 57%. At 1  $\mu$ M concentration, both IB-MECA and Thio-IB-MECA showed inhibitory effect of GW501516 by 14% and 22%, respectively, although the inhibition was not statistically significant. These result is similar with that of GSK0660, a PPAR $\delta$  antagonist, suggesting that IB-MECA and related A<sub>3</sub> AR ligands are PPAR $\delta$  antagonists (Fig. 10A, B). Next, the TR-FRET PPAR $\delta$  corepressor assay was carried out for the further investigation. PPAR $\delta$  agonists interfere with the interaction between PPAR $\delta$  and its corepressors such as silencing mediator of retinoid and thyroid hormone receptors (SMRT) (27). In this regard, under GW501516 co-existence condition or not, we analyzed whether compound **5** promote the interaction between PPAR $\delta$  and the labeled

corepressor peptide, which was derived from the interaction domain 2 (ID2) of SMRT (Fig. 10C). As expected, GW501516 decreased the recruitment of corepressor peptide to PPAR $\delta$  ligand-binding domain (Fig. 10C). GSK0660 and GSK3787, PPAR $\delta$  antagonists, significantly promoted the corepressive activity by the recruitment of SMRT-ID2, which was antagonized by GW501516. Importantly, similar to the effects of PPAR $\delta$  antagonists GSK0660 and GSK3787, the promotion of an interaction between PPAR $\delta$  and corepressor peptide by compound **5**, an A<sub>3</sub> AR antagonist, was concentration-dependent (Fig. 10D). A<sub>3</sub> AR agonist Thio-IB-MECA also enhanced the interaction in the TR-FRET PPAR $\delta$  corepressor assay system (Fig. 10D).

In mammalian cells, PPAR $\delta$  agonists increase the gene transcription of ANGPTL4 and PDK4 (28). To confirm that compound **5** is a PPAR $\delta$  antagonist, we measured ANGPTL4 and PDK4 mRNA levels during adipogenesis in hBM-MSCs (Fig. 11). Consistent with previous reports, the PPAR $\delta$  agonist GW501516 significantly increased ANGPTL4 and PDK4 gene transcription in the 3<sup>rd</sup> day after the induction of adipogenesis in hBM-MSCs (Fig. 11). Similar to the other PPAR $\delta$  antagonist, GSK0660, compound **5** did not affect ANGPTL4 and PDK4 mRNA levels in hBM-MSCs (Fig. 11). Recently, it was reported that the overexpression or transcriptional activation of PPAR $\delta$  inhibits PPAR $\gamma$  activity, suggesting the regulatory role of PPAR $\delta$  in PPAR $\gamma$  functions (29, 30). According to this, we tested the effects of PPAR $\delta$  antagonists GSK0660 and GSK3787 on hBM-MSC differentiation. Similar to compound **5**, both GSK0660 and GSK3787 promoted



adiponectin production during adipogenesis in hBM-MSCs in a concentration-dependent manner (Fig. 12). Conclusively, the adiponectin-promoting activity of IB-MECA and related A<sub>3</sub> AR ligands in hBM-MSCs is associated with both PPAR $\gamma$  partial agonism and PPAR $\delta$  antagonism. Taken together, IB-MECA and related A<sub>3</sub> AR ligands have a polypharmacophore of an A<sub>3</sub> AR ligand, a PPAR $\gamma$  partial agonist, and a PPAR $\delta$  antagonist.

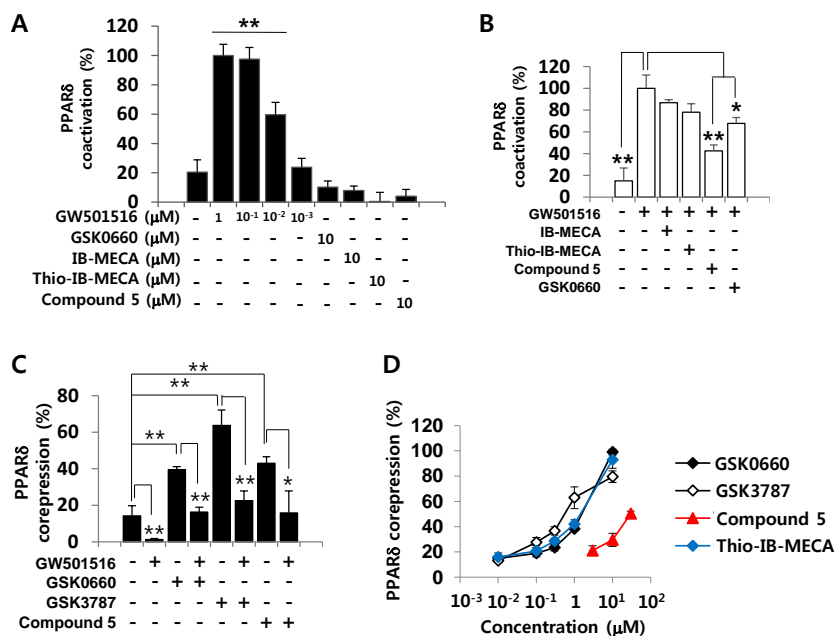


**Figure 10. PPAR $\delta$  coactivation and corepression activity of IB-MECA, Thio-IB-MECA and compound 5**

(A, B) TR-FRET PPAR $\delta$  coactivator assay was performed using fluorescein-C33 coactivator peptide. (B) The effects of IB-MECA, Thio-IB-MECA, compound 5, and GSK0660 (1  $\mu$ M) on the GW501516 (0.03  $\mu$ M)-induced interaction between fluorescein-C33 coactivator peptides and PPAR $\delta$  LBD in a TR-FRET PPAR $\delta$  coactivator assay were evaluated. (C) In a TR-FRET PPAR $\delta$  corepressor assay with SMRT-ID2 peptides, the activities of GSK0660, GSK3787, and compound 5 (1  $\mu$ M) were assessed in the condition that GW501516 (0.1  $\mu$ M) existed or not. (D) The ability of GSK0660, GSK3787, compound 5, and Thio-IB-MECA to recruit corepressors were determined. Results are the mean  $\pm$  SD (n = 3). \*  $p \leq 0.05$  and \*\*  $p \leq 0.01$ .

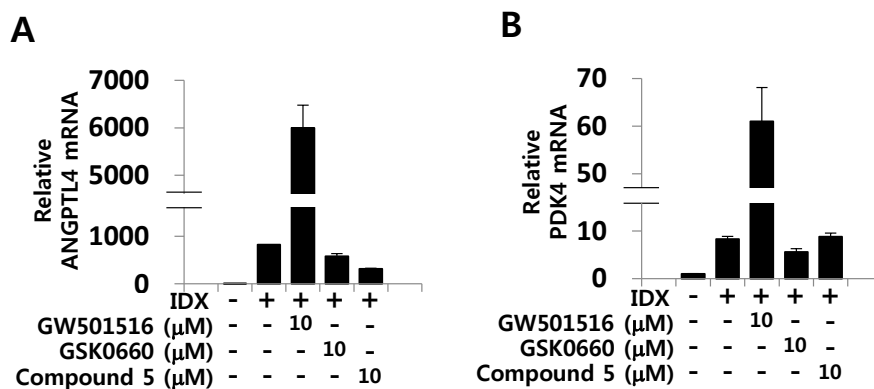


**Figure 11. Transcriptional expression profile of ANGPTL4 and PDK4 during adipogenesis in hBM-MSCs**

hBM-MSCs were differentiated in the IDX condition, and co-treated with GW501516, GSK0660, or compound **5** in the medium. On the 3<sup>rd</sup> day in culture, total RNA was extracted and Q-RT-PCR was performed for ANGPTL4 (A) and PDK4 (B). GAPDH was used as an internal control for Q-RT-PCR standardization. Results are the mean  $\pm$  SD of experiments using three independent hBM-MSCs (n = 3).

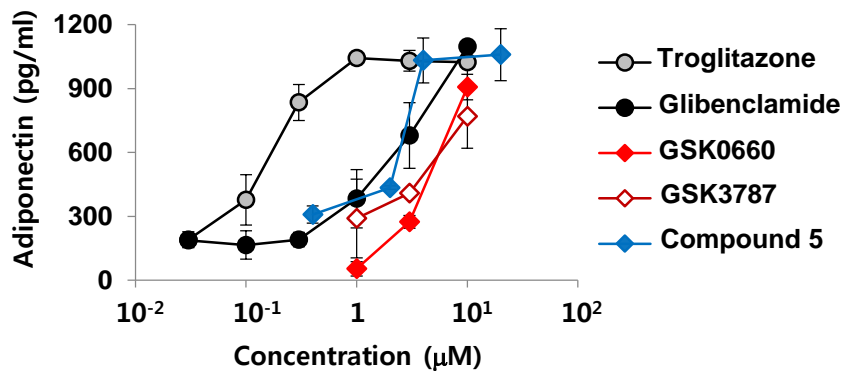


**Figure 12. The adiponectin-promoting effects of PPAR $\delta$  antagonists in hBM-MSCs**

As described in the materials and methods, adipogenesis was induced in the IDX condition with GSK0660, GSK3787, or compound **5** in hBM-MSCs for 7 days and ELISA was used to measure levels of adiponectin. All data represent averages of triplicates ( $\pm$  SD).

## **7. Polypharmacophore in IB-MECA and related A<sub>3</sub> AR ligands improves insulin sensitivity in STZ-induced diabetic mice.**

Based on the result that IB-MECA and related A<sub>3</sub> AR ligands significantly promoted adiponectin production in hBM-MSCs, they also might increase insulin sensitivity. However, the effects of IB-MECA and related A<sub>3</sub> AR ligands to promote insulin sensitivity has not been experimentally tested under *in vivo* conditions. Therefore, we evaluated the insulin-sensitizing effect of IB-MECA, Thio-IB-MECA, and compound **5** in the STZ-induced diabetes model in C57BL/6J mice (Fig. 13). In the STZ-induced diabetic mice, Thio-IB-MECA and compound **5** significantly decreased serum glucose levels suggesting insulin-sensitizing activity (Fig. 13A). IB-MECA tended to decrease serum glucose levels, although the result was not statistically significant (Fig. 13A). IB-MECA, Thio-IB-MECA, and compound **5** also significantly downregulated serum triglyceride levels in the diabetic mice model (Fig. 13B). In addition, compound **5** showed tendency to decrease the serum lactate levels in this model, but the effect was not significant (Fig. 13C). We also confirmed that the glucose-lowering effect of compound **5** in diabetic mice was dose-dependent (Fig. 14). Accordingly, a compound with a polypharmacological profile of an A<sub>3</sub> AR modulator, a PPAR $\gamma$  partial agonist, and a PPAR $\delta$  antagonist has insulin-sensitizing activity in STZ-induced diabetic mice.

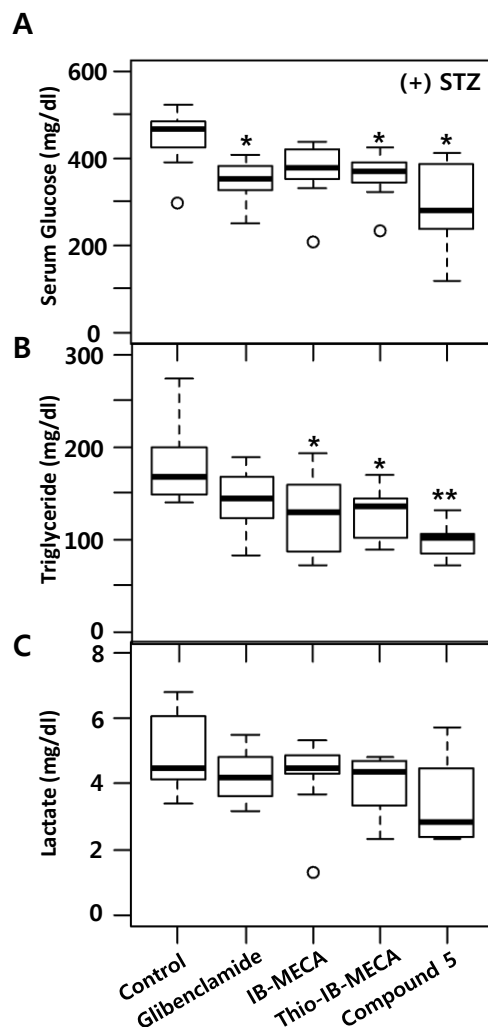


**Figure 13. Effects of IB-MECA, Thio-IB-MECA, and compound 5 on STZ-induced diabetic mice**

STZ-induced diabetic C57BL/6J mice were orally administered potential anti-diabetic drugs at 20 mg/ kg for 5 days. Glibenclamide was used as a positive control. Serum glucose (A), triglyceride (B) and lactate (C) levels were measured. Results are the mean  $\pm$  SD of experiments from seven independent donors. \*  $p \leq 0.05$  and \*\*  $p \leq 0.01$ .

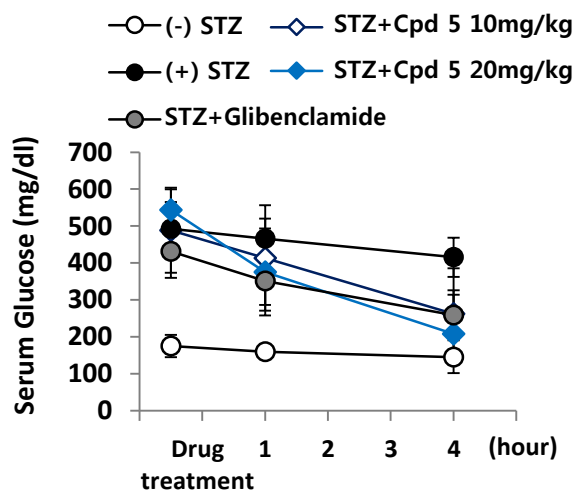


**Figure 14. The effects of compound 5 on serum glucose levels in STZ-induced diabetic mice**

On the 5<sup>th</sup> day of administration of compound (Cpd) 5, serum glucose concentrations were measured just before drug administration (0 hour), and at 1 and 4 hours after drug administration. Values are the mean  $\pm$  SD of experiments from seven independent donors.

## IV. Discussion

This study aimed to elucidate the role of ARs in adipogenesis regulation in hBM-MSCs based on the report that ARs regulate mammalian adipogenesis (15). By the pharmacological evaluation of A<sub>1</sub>, A<sub>2A</sub>, and A<sub>3</sub> AR agonists in hBM-MSCs, we found that only IB-MECA, an A<sub>3</sub> AR agonist, significantly promoted adiponectin production. In the human AR-transfected murine osteoblast precursor cell line 7F2, the AR agonists CCPA and NECA increased adipocyte differentiation by 20-30% in preadipocytes (15). However, in this study, both CCPA and NECA did not significantly promote adipogenesis in hBM-MSCs (Fig. 2A), implying that the AR signaling pathways differ between hMSCs and the murine 7F2 cell line. It was reported that transitional expression profile of AR subtypes changes after the induction of adipocyte differentiation from preadipocytes (31). Regarding this, the difference between the pharmacological outcomes of AR agonists on hBM-MSCs and those on the human AR-transfected 7F2 cell line may be partly explained by different lineage commitment stages for adipogenesis (32). Notably, compound **5**, an A<sub>3</sub> AR antagonist which is related to selective agonist Thio-Cl-IB-MECA by truncation at the 4'-carbon, showed similar characteristics to IB-MECA and other A<sub>3</sub> AR agonists in terms of promoting adipogenesis in hBM-MSCs. Therefore, we concluded that the IB-MECA-induced upregulation of adipogenesis is not specifically associated with the A<sub>3</sub> AR-mediated signaling pathway in hBM-MSCs. Although this study demonstrates that the AR signaling did not directly affect adipogenesis in hBM-MSCs, ARs may regulate adipocyte functions in adipose



tissue. Recent studies showed that the A<sub>1</sub> AR regulates lipolysis and lipogenesis in A<sub>1</sub> AR knockout mice and A<sub>2A</sub> AR agonists increased energy expenditure in brown adipose tissue (BAT) (33-35). Because the adipogenic condition for hBM-MSCs is preferential to generate white adipose tissue cells, it may not correspond to BAT study. Further studies are needed to elucidate the role of ARs in human adipocyte function or BAT differentiation.

We described that IB-MECA and related A<sub>3</sub> AR ligands interact with multiple pharmacological targets: A<sub>3</sub> AR, PPAR $\gamma$ , and PPAR $\delta$ . These A<sub>3</sub> AR modulators partially transactivated PPAR $\gamma$  and simultaneously antagonized PPAR $\delta$ . Partial PPAR $\gamma$  agonists improve pathologic parameters in human metabolic diseases (36). The insulin-sensitizing effects of PPAR $\delta$  antagonists are controversial (37). Recent reports indicated that PPAR $\delta$  overexpression or transcriptional activation inhibits PPAR $\gamma$  activity (29, 30). Therefore, by blocking the inhibitory effect of PPAR $\delta$  on PPAR $\gamma$  transactivation, the PPAR $\delta$  antagonistic activity of IB-MECA and related A<sub>3</sub> AR ligands may improve insulin sensitivity. In fact, the polypharmacological outcome of IB-MECA and related A<sub>3</sub> AR ligands for adiponectin production is primarily dependent on the binding activity to the nuclear transcription factors PPAR $\gamma$  and PPAR $\delta$ . Regardless of A<sub>3</sub> AR agonists or antagonists, IB-MECA and the related A<sub>3</sub> AR ligands promoted adiponectin production in hBM-MSCs and improved glucose-lowering effects in STZ-induced diabetic C57BL6/J mice. The anti-diabetic potential of IB-MECA and related A<sub>3</sub> AR ligands may be due to their effect on both PPAR $\gamma$  and PPAR $\delta$ . Structurally, this polypharmacophore encompasses adenosine-5'-uronamides and its 4'-truncated derivatives that also

have bulky hydrophobic substitutions at the N<sup>6</sup> position, such as halobenzyl. Thio-CI-IB-MECA was the most potent inhibitor at PPAR $\delta$  among A<sub>3</sub> AR agonists (Table 4). Extension of the 5'-uronamide group with alkyl or cycloalkyl substituents did not reduce the inhibitor potency at PPAR $\delta$  compared to Thio-IB-MECA. Among truncated derivatives, all of which were thionucleosides, the two most potent compounds at PPAR $\delta$  were N<sup>6</sup>-3-iodobenzyl derivative **5** and N<sup>6</sup>-3-chlorobenzyl derivative **6**.

The concept of polypharmacology defines a single drug molecule with multiple drug targets to treat complex diseases with polygenic etiology (38, 39). For instance, a single drug molecule interacting with multiple kinases in dysregulated cancer cells has provided experimental evidence of the effectiveness of the polypharmacology approach (1, 40). The effects of IB-MECA and CI-IB-MECA, referred to as CF101 and CF102 respectively in clinical trials, have been evaluated in cancer, psoriasis, rheumatoid arthritis, and dry eye syndrome (41). However, the A<sub>3</sub> AR-mediated pharmacology alone cannot fully explain these diverse clinical activities of IB-MECA and CI-IB-MECA. The anti-cancer effects of IB-MECA and CI-IB-MECA are showed in various human cancerous tumors such as melanoma, lymphoma, colon carcinoma and hepatocellular carcinoma (42-45). In contrast, other studies indicates that IB-MECA and CI-IB-MECA have A<sub>3</sub> AR-independent anti-cancer mechanisms in various cancer cell lines (43, 45). Our findings suggest the existence of an alternative A<sub>3</sub> AR-independent anti-cancer mechanism for IB-MECA and CI-IB-MECA, i.e. regulation of both PPAR $\gamma$  and PPAR $\delta$ . There are supporting evidences that the ligand-induced PPAR $\gamma$  activation

could lead to apoptosis of cancer cells, and a PPAR $\delta$  antagonist inhibits the cancer cell growth whereas the PPAR $\delta$  agonist GW501516 promotes the tumorigenesis of some cancer cell lines in animal models (48-50). In this regard, the anti-cancer activity of IB-MECA and Cl-IB-MECA must be explained with their polypharmacological characteristics of an A<sub>3</sub> AR agonist, a PPAR $\gamma$  partial agonist, and a PPAR $\delta$  antagonist. The polypharmacological context of A<sub>3</sub> AR, PPAR $\gamma$ , and PPAR $\delta$  in human cancers may provide therapeutic benefits in the future clinical development of IB-MECA and related A<sub>3</sub> AR ligands as anti-cancer drugs.

IB-MECA and Cl-IB-MECA also have been clinically evaluated for the treatment of human inflammatory diseases such as rheumatoid arthritis and psoriasis (11, 41). The polypharmacological characteristics of IB-MECA and related A<sub>3</sub> AR ligands also provides a good mechanistic explanation for anti-inflammatory activity. PPAR $\gamma$  agonists inhibit pro-inflammatory cytokine production from monocytes or macrophages, and their PPAR $\gamma$  expression is correlated with the disease severity in rheumatoid arthritis (51). A study showed that the PPAR $\gamma$  agonist pioglitazone mildly improved the pathological symptoms of rheumatoid arthritis in a randomized clinical trial (52). In animal models with psoriatic conditions, the inhibition of PPAR $\delta$  by selective antagonists such as GSK0660 and GSK3787 improve inflammation (53). Therefore, to explain the anti-inflammatory activity of IB-MECA and related A<sub>3</sub> AR ligands in various clinical conditions, it is necessary to address the possible involvement of not only A<sub>3</sub> AR- and PPAR $\gamma$ -, but also PPAR $\delta$ -mediated pathways in their *in vivo* anti-inflammatory outcomes.

This study emphasized that the anti-diabetic potential of IB-MECA and related A<sub>3</sub> AR ligands is associated with undiscovered interactions, i.e. both PPAR $\gamma$  partial agonism and PPAR $\delta$  antagonism. To develop these compounds as anti-type II diabetes drugs further studies to address clinical efficacy or toxicity will be necessary depending on their A<sub>3</sub> AR agonist or A<sub>3</sub> AR antagonist activity. In addition, when IB-MECA and related A<sub>3</sub> AR ligands are clinically developed as A<sub>3</sub> AR modulators to treat A<sub>3</sub> AR-associated diseases, the adverse effects or clinical benefits induced from PPAR $\gamma$  partial agonism and PPAR $\delta$  antagonism should be considered. Up to now, most polypharmacology case studies demonstrated the limited molecular targets to a structurally similar protein family, such as multiple tyrosine kinases (1, 40). However, in this study, IB-MECA provides a good case study for a single drug molecule simultaneously targeting different protein families: the GPCR and NR families. One of the technical goals of systems pharmacology is defining polypharmacology in the context of the accurate prediction of clinical efficacy and safety. Therefore, more evidence on a single drug molecule modulating multi-targets in different protein families must be presented to accomplish the goal. In this context, the polypharmacological characteristics of IB-MECA and related A<sub>3</sub> AR ligands can provide therapeutic insight into their multi-purpose efficacy to various human diseases such as type II diabetes, cancers, rheumatoid arthritis, and psoriasis.

## V. Reference

1. Gujral TS, Peshkin L, Kirschner MW (2014) Exploiting polypharmacology for drug target deconvolution. *Proc Natl Acad Sci USA* 111(13):5048-5053.
2. Moffat JG, Rudolph J, Bailey D (2014) Phenotypic screening in cancer drug discovery - past, present and future. *Nat Rev Drug Discov* 13(8):588-602.
3. Noh M (2012) Interleukin-17A increases leptin production in human bone marrow mesenchymal stem cells. *Biochem Pharmacol* 83(5):661-670.
4. Shin DW, et al. (2009) (-)-Catechin promotes adipocyte differentiation in human bone marrow mesenchymal stem cells through PPAR gamma transactivation. *Biochem Pharmacol* 77(1):125-133.
5. Finucane FM, et al. (2009) Correlation of the leptin:adiponectin ratio with measures of insulin resistance in non-diabetic individuals. *Diabetologia* 52(11):2345-2349.
6. Shetty S, Kusminski CM, Scherer PE (2009) Adiponectin in health and disease: evaluation of adiponectin-targeted drug development strategies. *Trends Pharmacol Sci* 30(5):234-239.
7. Fukuen S, et al. (2005) Sulfonylurea agents exhibit peroxisome proliferator-activated receptor gamma agonistic activity. *J Biol Chem* 280(25):23653-23659.

8. Kellinsalmi M, et al. (2007) Inhibition of cyclooxygenase-2 down-regulates osteoclast and osteoblast differentiation and favours adipocyte formation in vitro. *Eur J Pharmacol* 572(2-3):102-110.
9. Lehmann JM, Lenhard JM, Oliver BB, Ringold GM, Kliewer SA (1997) Peroxisome proliferator-activated receptors alpha and gamma are activated by indomethacin and other non-steroidal anti-inflammatory drugs. *J Biol Chem* 272(6):3406-3410.
10. Byun Y, et al. (2013) The opposite effect of isotype-selective monoamine oxidase inhibitors on adipogenesis in human bone marrow mesenchymal stem cells. *Bioorg Med Chem Lett* 23(11):3273-3276.
11. Jacobson KA, Gao ZG (2006) Adenosine receptors as therapeutic targets. *Nat Rev Drug Discov* 5(3):247-264.
12. Silverman MH, et al. (2008) Clinical evidence for utilization of the A<sub>3</sub> adenosine receptor as a target to treat rheumatoid arthritis: data from a phase II clinical trial. *J Rheumatol* 35(1):41-48.
13. Biaggioni I, Paul S, Puckett A, Arzubiaga C (1991) Caffeine and theophylline as adenosine receptor antagonists in humans. *J Pharmacol Exp Ther* 258(2):588-593.
14. Su SH, et al. (2013) Caffeine inhibits adipogenic differentiation of primary adipose-derived stem cells and bone marrow stromal cells. *Toxicol In Vitro* 27(6):1830-1837.

15. Gharibi B, Abraham AA, Ham J, Evans BA (2012) Contrasting effects of A<sub>1</sub> and A<sub>2b</sub> adenosine receptors on adipogenesis. *Int J Obes (Lond)* 36(3):397-406.
16. He W, Mazumder A, Wilder T, Cronstein BN (2013) Adenosine regulates bone metabolism via A<sub>1</sub>, A<sub>2A</sub>, and A<sub>2B</sub> receptors in bone marrow cells from normal humans and patients with multiple myeloma. *FASEB J* 27(9):3446-3454.
17. Johansson SM, et al. (2007) A<sub>1</sub> receptor deficiency causes increased insulin and glucagon secretion in mice. *Biochem Pharmacol* 74(11):1628-1635.
18. Johnston-Cox H, et al. (2012) The A<sub>2b</sub> adenosine receptor modulates glucose homeostasis and obesity. *PloS one* 7(7):e40584.
19. Choi WJ, et al. (2009) Design and synthesis of N(6)-substituted-4'-thioadenosine-5'-uronamides as potent and selective human A<sub>3</sub> adenosine receptor agonists. *Bioorg Med Chem* 17(23):8003-8011.
20. Jeong LS, et al. (2007) Discovery of a new nucleoside template for human A<sub>3</sub> adenosine receptor ligands: D-4'-thioadenosine derivatives without 4'-hydroxymethyl group as highly potent and selective antagonists. *J Med Chem* 50(14):3159-3162.
21. Jeong LS, et al. (2008) Structure-activity relationships of truncated D- and 1-4'-thioadenosine derivatives as species-independent A<sub>3</sub> adenosine receptor antagonists. *J Med Chem* 51(20):6609-6613.
22. Chang C, et al. (1999) Dissection of the LXXLL nuclear receptor-coactivator interaction motif using combinatorial peptide libraries: discovery of peptide

antagonists of estrogen receptors alpha and beta. *Mol Cell Endocrinol* 19(12):8226-8239.

23. Chen JD, Evans RM (1995) A transcriptional co-repressor that interacts with nuclear hormone receptors. *Nature* 377(6548):454-457.

24. Pfaffl MW, Horgan GW, Dempfle L (2002) Relative expression software tool (REST) for group-wise comparison and statistical analysis of relative expression results in real-time PCR. *Nucleic Acids Res* 30(9):e36.

25. Rosen ED, MacDougald OA (2006) Adipocyte differentiation from the inside out. *Nat Rev Mol Cell Biol* 7(12):885-896.

26. Choi JH, et al. (2010) Anti-diabetic drugs inhibit obesity-linked phosphorylation of PPARgamma by Cdk5. *Nature* 466(7305):451-456.

27. Yu S, Reddy JK (2007) Transcription coactivators for peroxisome proliferator-activated receptors. *Biochim Biophys Acta* 1771(8):936-951.

28. Shearer BG, et al. (2008) Identification and characterization of a selective peroxisome proliferator-activated receptor beta/delta (NR1C2) antagonist. *Mol Endocrinol* 22(2):523-529.

29. Shi Y, Hon M, Evans RM (2002) The peroxisome proliferator-activated receptor delta, an integrator of transcriptional repression and nuclear receptor signaling. *Proc Natl Acad Sci USA* 99(5):2613-2618.

30. Zuo X, et al. (2006) Oxidative metabolism of linoleic acid modulates PPAR-beta/delta suppression of PPAR-gamma activity. *Oncogene* 25(8):1225-1241.



31. Borglum JD, et al. (1996) Changes in adenosine A<sub>1</sub>- and A<sub>2</sub>-receptor expression during adipose cell differentiation. *Mol Cell Endocrinol* 117(1):17-25.
32. Pittenger MF, et al. (1999) Multilineage potential of adult human mesenchymal stem cells. *Science* 284(5411):143-147.
33. Johansson SM, Lindgren E, Yang JN, Herling AW, Fredholm BB (2008) Adenosine A<sub>1</sub> receptors regulate lipolysis and lipogenesis in mouse adipose tissue-interactions with insulin. *Eur J Pharmacol* 597(1-3):92-101.
34. LaNoue KF, Martin LF (1994) Abnormal A<sub>1</sub> adenosine receptor function in genetic obesity. *FASEB J* 8(1):72-80.
35. Gnad T, et al. (2014) Adenosine activates brown adipose tissue and recruits beige adipocytes via A<sub>2A</sub> receptors. *Nature* 516(7531):395-399.
36. Burgermeister E, et al. (2006) A novel partial agonist of peroxisome proliferator-activated receptor-gamma (PPARgamma) recruits PPARgamma-coactivator-1alpha, prevents triglyceride accumulation, and potentiates insulin signaling in vitro. *Mol Endocrinol* 20(4):809-830.
37. Tanaka T, et al. (2003) Activation of peroxisome proliferator-activated receptor delta induces fatty acid beta-oxidation in skeletal muscle and attenuates metabolic syndrome. *Proc Natl Acad Sci USA* 100(26):15924-15929.
38. Anighoro A, Bajorath J, Rastelli G (2014) Polypharmacology: challenges and opportunities in drug discovery. *J Med Chem* 57(19):7874-7887.

39. Hopkins AL (2008) Network pharmacology: the next paradigm in drug discovery. *Nat Chem Biol* 4(11):682-690.
40. Dar AC, Das TK, Shokat KM, Cagan RL (2012) Chemical genetic discovery of targets and anti-targets for cancer polypharmacology. *Nature* 486(7401):80-84.
41. Fishman P, Bar-Yehuda S, Liang BT, Jacobson KA (2012) Pharmacological and therapeutic effects of A<sub>3</sub> adenosine receptor agonists. *Drug Discov Today* 17(7-8):359-366.
42. Bar-Yehuda S, et al. (2005) CF101, an agonist to the A<sub>3</sub> adenosine receptor, enhances the chemotherapeutic effect of 5-fluorouracil in a colon carcinoma murine model. *Neoplasia* 7(1):85-90.
43. Lu J, Pierron A, Ravid K (2003) An adenosine analogue, IB-MECA, down-regulates estrogen receptor alpha and suppresses human breast cancer cell proliferation. *Cancer Res* 63(19):6413-6423.
44. Madi L, et al. (2004) The A<sub>3</sub> adenosine receptor is highly expressed in tumor versus normal cells: potential target for tumor growth inhibition. *Clin Cancer Res* 10(13):4472-4479.
45. Morello S, et al. (2008) CI-IB-MECA inhibits human thyroid cancer cell proliferation independently of A<sub>3</sub> adenosine receptor activation. *Cancer Biol Ther* 7(2):278-284.
48. Youssef J, Badr M (2011) Peroxisome proliferator-activated receptors and cancer: challenges and opportunities. *Br J Pharmacol* 164(1):68-82.

49. Zaveri NT, et al. (2009) A novel peroxisome proliferator-activated receptor delta antagonist, SR13904, has anti-proliferative activity in human cancer cells. *Cancer Biol Ther* 8(13):1252-1261.
50. Gupta RA, et al. (2004) Activation of nuclear hormone receptor peroxisome proliferator-activated receptor-delta accelerates intestinal adenoma growth. *Nat Med* 10(3):245-247.
51. Palma A, et al. (2012) Peroxisome proliferator-activated receptor-gamma expression in monocytes/macrophages from rheumatoid arthritis patients: relation to disease activity and therapy efficacy--a pilot study. *Rheumatology (Oxford)* 51(11):1942-1952.
52. Ormseth MJ, et al. (2013) Peroxisome proliferator-activated receptor gamma agonist effect on rheumatoid arthritis: a randomized controlled trial. *Arthritis Res Ther* 15(5):R110.
53. Hack K, et al. (2012) Skin-targeted inhibition of PPAR beta/delta by selective antagonists to treat PPAR beta/delta-mediated psoriasis-like skin disease in vivo. *PloS one* 7(5):e37097.

요약 (국문초록)

# 사람의 중간엽줄기세포에서 지방분화 조절 물질의 타겟 규명

안 세 연

서울대학교 약학대학원

제약학과 천연물과학 전공

표현형 기반 신약평가모델은 분자 타겟 기반 전략의 대안으로 현대의 신약개발에서 각광받고 있다. 사람의 중간엽줄기세포의 지방세포분화 유도를 통한 표현형 평가는 대사성 질환 조절 물질의 평가모델로 활용되고 있다. 본 실험모델에서 지방세포의 아디포넥틴 분비는 인슐린 감수성과 밀접한 연관이 있다. 따라서 사람의 중간엽줄기세포에서 지방분화를 유도하고 아디포넥틴 분비를 촉진시키는 물질의 타겟 규명은 당뇨, 비만, 고지혈증과 같은 대사성 질환의 조절 기작을 밝히는 데 연구가치가 있다.

A<sub>3</sub> 아데노신 수용체 (AR) 의 리간드로 알려진 IB-MECA 가 중간엽줄기세포에서 지방분화를 촉진시키는 사실을 실험적으로 밝혔다. 나아가 IB-MECA 와 구조 유사체들의 중간엽줄기세포에서 지방분화

촉진능과 아디포넥틴 분비능을 평가하였다. 본 물질들이 페록시솜증식체활성화수용체 (PPAR) $\gamma$ 의 부분효능제이면서 PPAR $\delta$ 의 길항제임을 실험적으로 입증했고, 두 가지 수용체의 결합능과 아디포넥틴 촉진능 사이에 양의 상관관계가 존재함을 통계적으로 분석했다. 결과적으로 A<sub>3</sub> AR, PPAR $\gamma$ , 그리고 PPAR $\delta$ 에 모두 결합하는 특성을 고려해, 다중약리학의 개념이 적용된 새로운 대사성질환 조절 물질로서의 가능성을 제시했다. 또한 스트렙토조토신 유도 당뇨 쥐 실험을 통해 가장 강력한 지방분화효능을 보인 IB-MECA의 유도체가 혈당과 혈중 중성지방 수치를 개선한다는 사실을 확인했다.

본 연구는 중간엽줄기세포의 표현형 기반 타겟 연구를 통해 IB-MECA의 지방분화 촉진 기전을 밝히고, 대사성질환의 조절에 새로운 방향성을 제시한다. 또한 다중약리학적 관점에서 핵수용체와 G 단백질 연결 수용체에 모두 작용하는 다중타겟 규명 연구를 통해, 대사성질환 조절 신약개발을 위한 새로운 접근법을 제시했다는 것에 의의가 있다.

**주요어 :** 다중약리학, IB-MECA, 사람의 중간엽줄기세포, 표현형 평가, 타겟 규명, 지방분화

**학번 :** 2015-21884